Electronic Supplementary Material (ESI) for Polymer Chemistry.

Role of Pendant Side-Chain Length in Determining Polymer 3D Printability

Tanmay Jain,[a] William Clay,[a,b] Yen-Ming Tseng,[a] Apoorva Viswakarma,[a] Amal Narayanan,[a] Deliris Ortiz,[a] Qianhui Liu,[a] Abraham Joy[a*]

[a] *Department of Polymer Science, The University of Akron, 170 University Avenue, Akron, Ohio, 44325*
[b] *Department of Chemistry & Biochemistry, The University of Mount Union, 1972 Clark Avenue, Alliance, OH, 44601*
** abraham@uakron.edu.*

Contents:

1. ^{1}H NMR Spectroscopies of monomers

a. N,N-bis(2-hydroxyethyl)propionamide (**mC_2**)

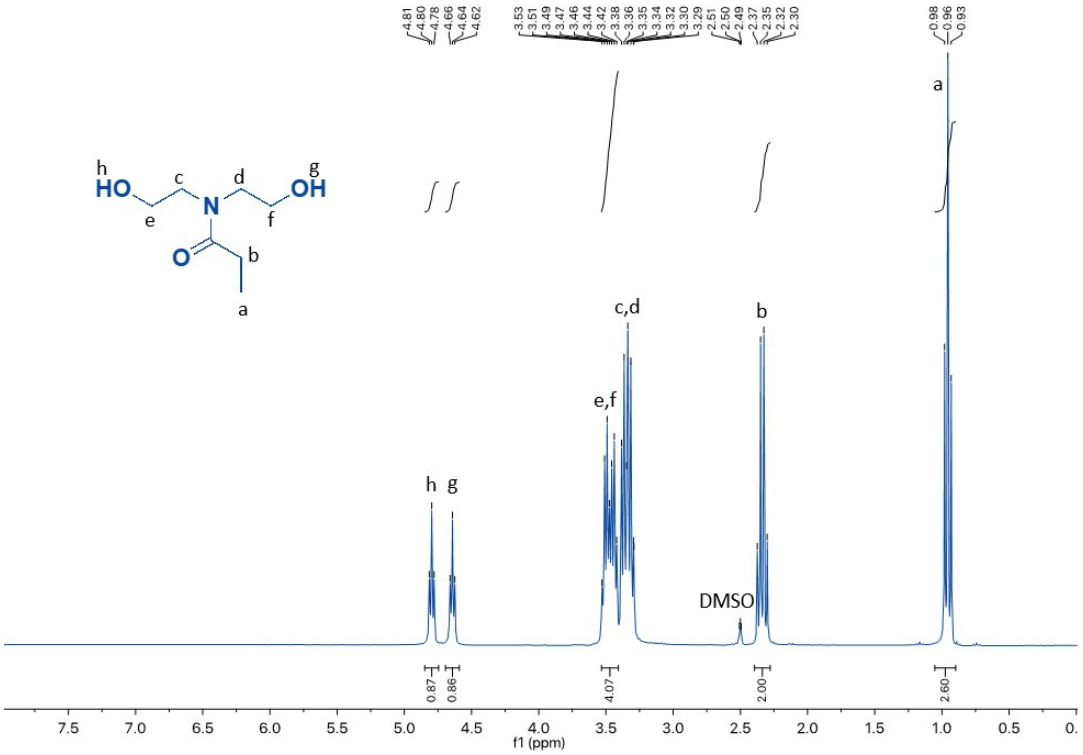

b. N,N-bis(2-hydroxyethyl)heptanamide (**mC_6**)

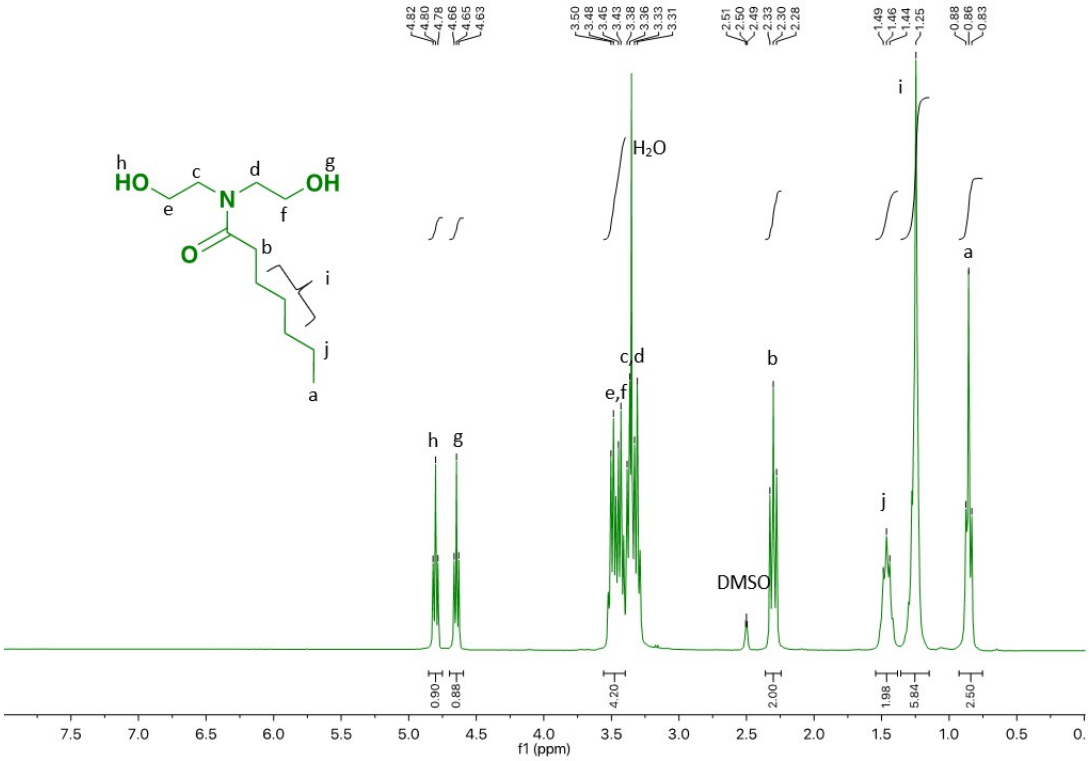

c. N,N-bis(2-hydroxyethyl)palmitamide (**mC$_{15}$**)

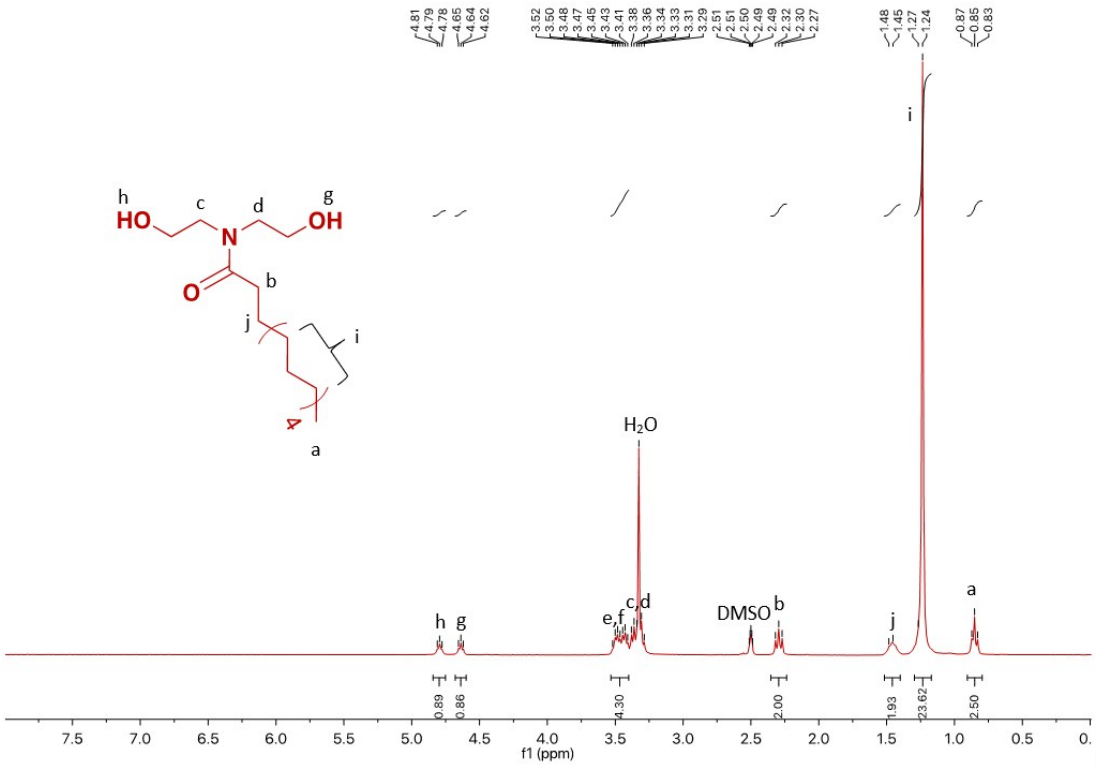

Figure S1: ^{1}H – NMR of the **mC$_2$**, **mC$_6$**, and **mC$_{15}$** monomers.

2. DSC thermogram of the polyesters

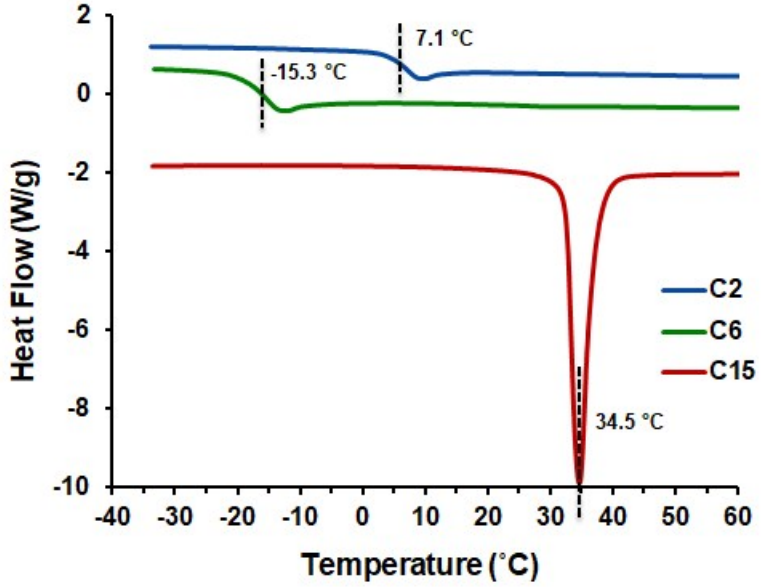

Figure S2: DSC thermogram to show the glass transition temperature (T_g) for the **C$_2$** and **C$_6$** polyester and the melting temperature (T_m) for the **C$_{15}$** polymer.

3. **DSC thermogram of the cooling cycle of the C_{15} polyester**

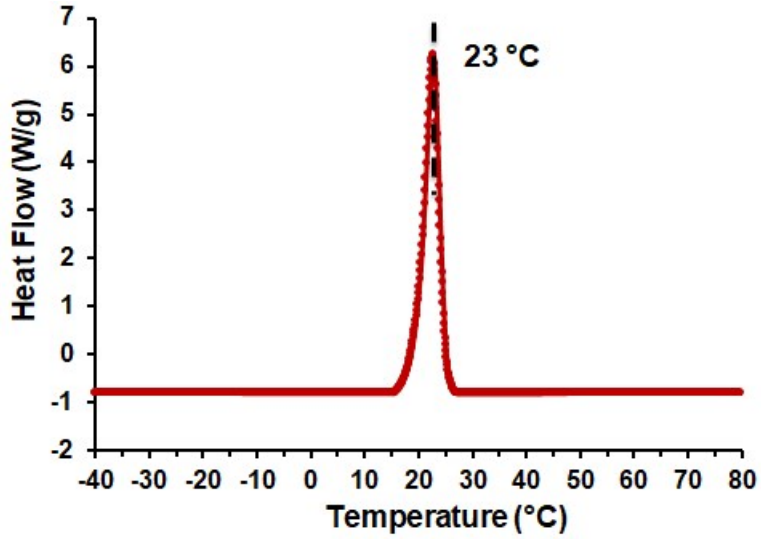

Figure S3: DSC thermogram to show the recrystallization temperature (T_c) for the **C_{15}** polyester.

4. **Stress relaxation plot of a general polymer**

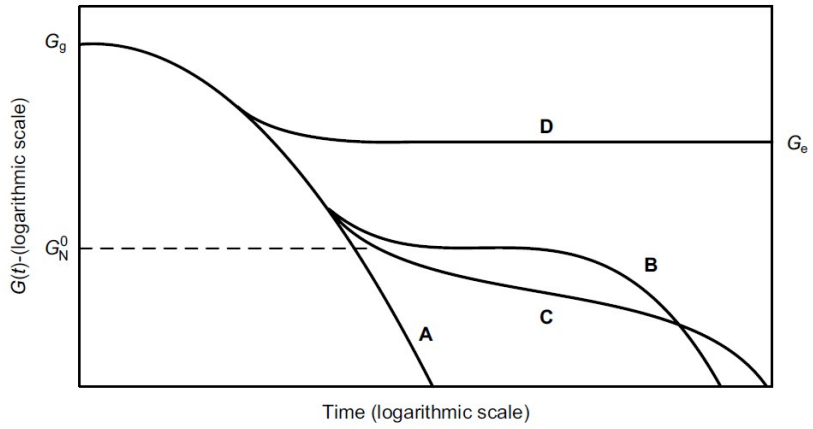

Figure S4: Relaxation modulus of four samples of a linear polymer – A) unentangled molten polymer, B) monodispersed, entangled molten polymer, C) polydispersed, entangled molten polymer, and D) crosslinked elastomer.[1]

5. Fitting stress relaxation to discrete relaxation model

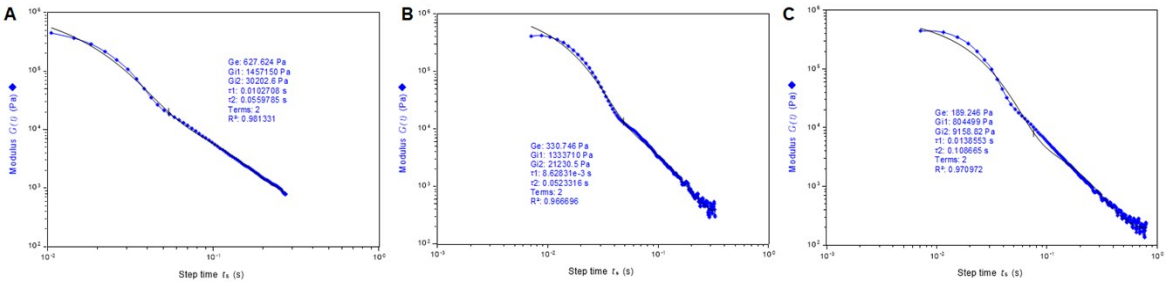

Figure S5.A: Fitting discrete relaxation model to the $\mathbf{C_2}$ stress relaxation at 50 °C. The experiment was performed in triplicate- A) Trial 1, B) Trial 2, and C) Trial 3.

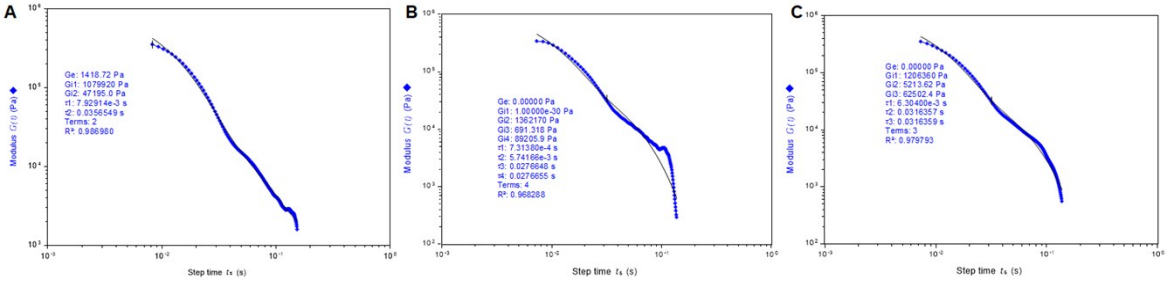

Figure S5.B: Fitting discrete relaxation model to the $\mathbf{C_6}$ stress relaxation at 25 °C. The experiment was performed in triplicate- A) Trial 1, B) Trial 2, and C) Trial 3.

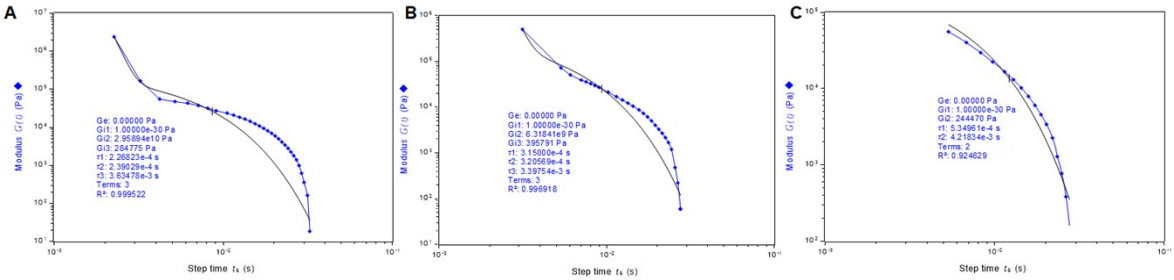

Figure S5.C: Fitting discrete relaxation model to the $\mathbf{C_{15}}$ stress relaxation at 35 °C. The experiment was performed in triplicate- A) Trial 1, B) Trial 2, and C) Trial 3.

Polymer	τ (trial 1) [sec]	τ (trial 2) [sec]	τ (trial 3) [sec]	τ (average) [sec]	std. error
$\mathbf{C_2}$	0.0662493	0.06095991	0.1225203	0.083243	0.019698
$\mathbf{C_6}$	0.04358404	0.06180334	0.0695756	0.058321	0.007702
$\mathbf{C_{15}}$	0.003872975	0.004033109	0.0047326	0.004213	0.000264

Table S1: Relaxation times for $\mathbf{C_2}$ at 50°C, $\mathbf{C_6}$ at 25°C, and $\mathbf{C_{15}}$ at 35°C.

6. **Filament extrusion test**

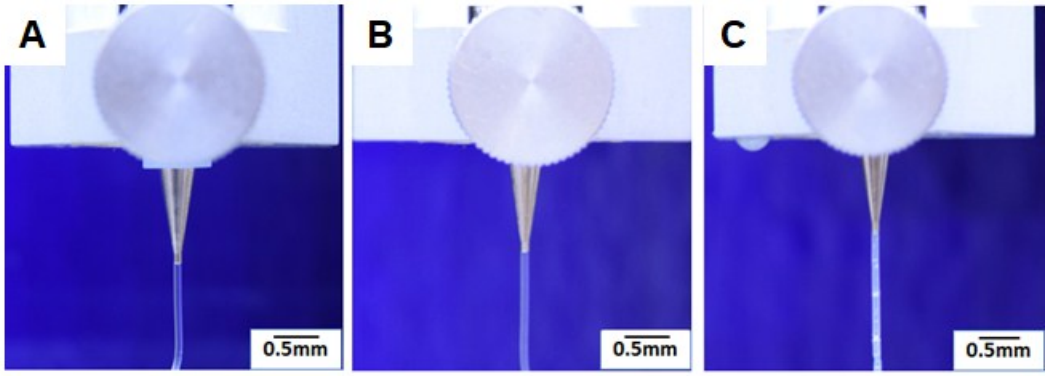

Figure S6: Continuous filament extrusion of the A) $\mathbf{C_2}$, B) $\mathbf{C_6}$, and $\mathbf{C_{15}}$ polyesters at temperatures 50 °C, 25 °C, 35 °C and pressures of 250kPa, 250kPa, and 40 kPa, respectively.

7. **Elastic modulus G' Vs Temperature**

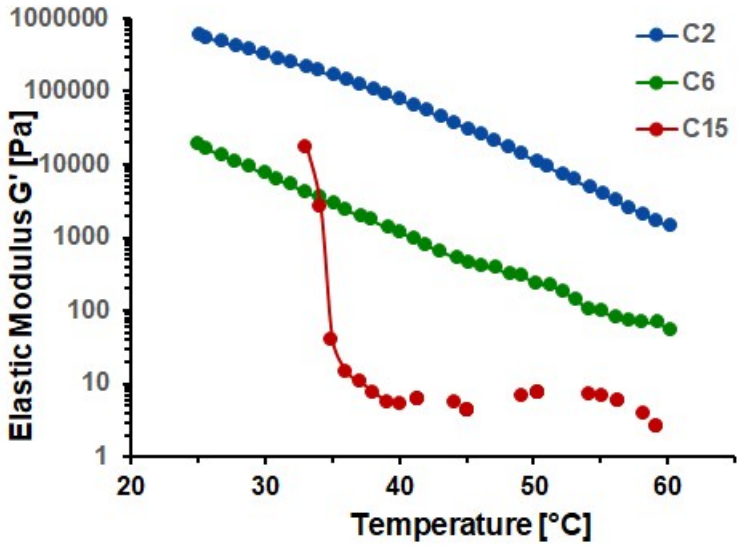

Figure S7: Elastic modulus (G') of the synthesized polyesters as a function of temperature determined by small amplitude oscillatory measurement.

8. NIH 3T3 fibroblasts cell viability

Mouse fibroblast NIH-3T3 cells (ATCC CRL-1658) were purchased from ATCC and were cultured using DMEM medium supplemented with 10% FBS and 1% penicillin streptomycin. The cells were grown at 37 °C in 5% CO_2 until reaching ~ 90% confluency. The cells were harvested using 0.25% trypsin solution and seeded onto the polymer coated coverslips and the blank coverslips in a 24 well plate at a density of 5000 cells/cm^2. The cells were incubated for 24 and 72 hrs before determining viability using a Pierce LDH Cytotoxicity Assay Kit, according to the instructions of the manufacturer.

9. Static contact angle

Polymer thin films were coated on pre-cleaned silicon wafers from 4% (w/v) chloroform solutions. Contact angle of three liquids of known surface tension (ethylene glycol, propylene glycol, and water) on the polymer films were measured using a Ramé-Hart contact angle goniometer. The measurements were conducted under room temperature. The static water contact angle measurements are shown in Figure S9.

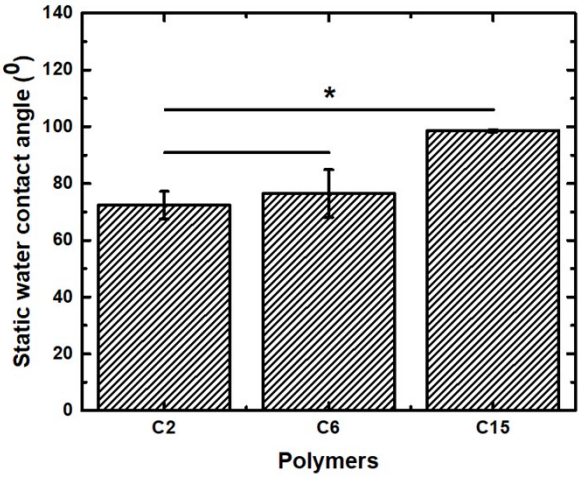

Figure S8: Static water contact angle of the synthesized polyesters. The data represented here are presented as mean ± standard deviation (SD) and '*' represents the statistical significance among the samples using Tukey mean comparison test ($p < 0.05$). Error bars (SD) are evaluated using at least 3 measurements for each polymer.

10. Surface energy characterization

The surface energy plays an important role in determining cell – biomaterial interactions.[2,3] Surface energy of material can be estimated from the contact angle measurements.[4,5] The following equation was used to calculate the surface energy of the polyesters[6]-

$$\frac{(1+\cos\theta_{LP})\gamma_L}{2\sqrt{\gamma_L^d}} = \sqrt{\gamma_P^d} + \sqrt{\frac{\gamma_L^p}{\gamma_L^d}}\sqrt{\gamma_P^p} \qquad (1)$$

Where θ_{LP} is the Young's contact angle, $\gamma_L$is the liquid surface tension, γ_L^d is the dispersion component of the liquid surface tension, γ_L^p is the polar component of the liquid surface tension, γ_P^d is the dispersion component and γ_P^p is the polar component of the polymer surface energy. The dispersion and polar components of polymer surface energy can be obtained from the slope and intercept of fitting the contact angle data with various liquids into equation 1. Water, ethylene glycol, and propylene glycol was used for this study. Their surface tension values can be found elsewhere.[6–8] The results of the contact angle measurements are plotted according to equation 1 in Figure S9. The surface energies are summarized in Table S2.

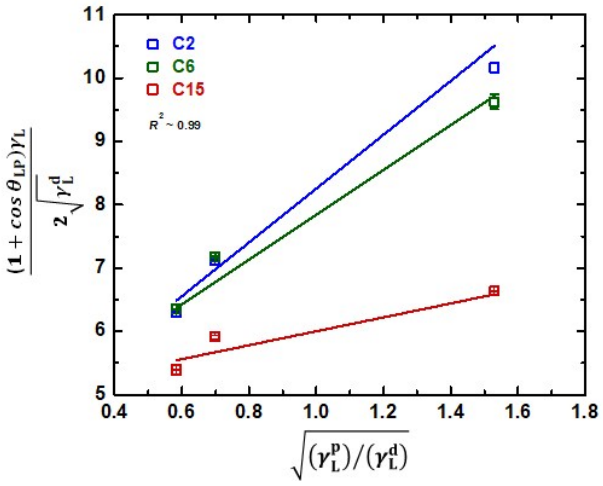

Figure S9: Surface energy fitting plots derived from contact angle measurements.

Table S2: Surface energies of the polyesters.

Polymer	γ_P^p (mJ/m^2)	γ_P^d (mJ/m2)	γ_P (mJ/m2)
C_2	18.1 ± 0.4	16.0 ± 0.0	34.1 ± 0.0
C_6	12.5 ± 0.2	18.5 ± 0.4	31.0 ± 0.0
C_{15}	1.21 ± 0.2	24.0 ± 0.6	25.2 ± 0.1

Table **S1** summarizes the polar (γ_P^p), dispersive (γ_P^d), and total surface energies (γ_P) of each polymer. The γ_P^p of C_2 and C_6 are comparable to their corresponding γ_P^d. Interestingly, for C_{15}, γ_P^d was found to be ~ 20 times higher than γ_P^p due to the dominating non-polar nature of C_{15} chains compared to C_6 and C_2.

11. GPC traces for C_2, C_6, and C_{15} polyesters

C_2 polyester:

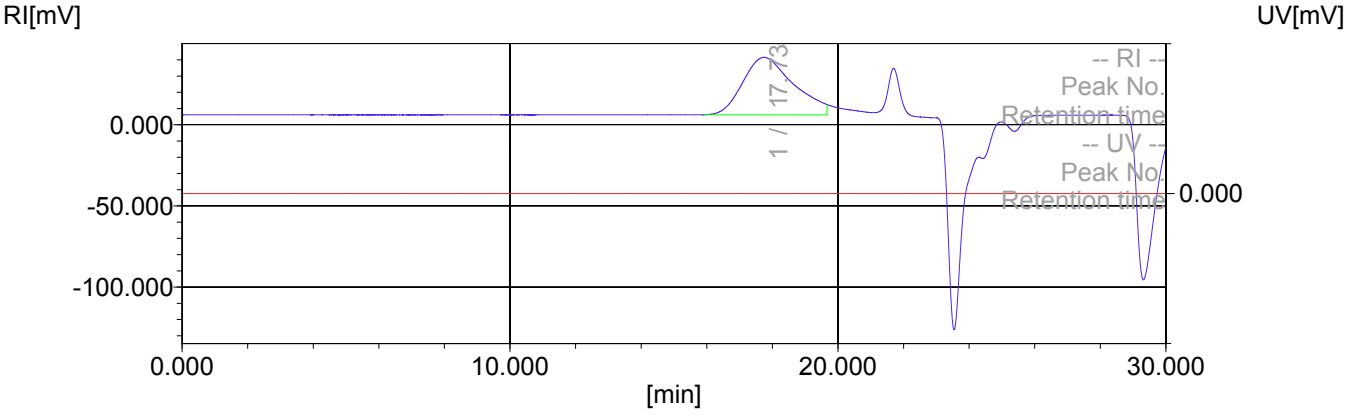

Result of molecular weight calculation (RI)

Peak 1 Valley Peak

	[min]	[mV]	[mol]		
Peak start	15.888	6.196	54,735	Mn	6,198
Peak top	17.735	41.558	10,436	Mw	10,271
Peak end	19.670	12.429	1,440	Mz	14,919
				Mz+1	19,385
				Mv	10,271
Height [mV]			35.470	Mp	10,733
Area [mV*sec]			3826.242	Mz/Mw	1.452
Height% [%]			100.000	Mw/Mn	1.657
[eta]			10271.40765	Mz+1/Mw	1.887

C_6 polyester:

[mV]

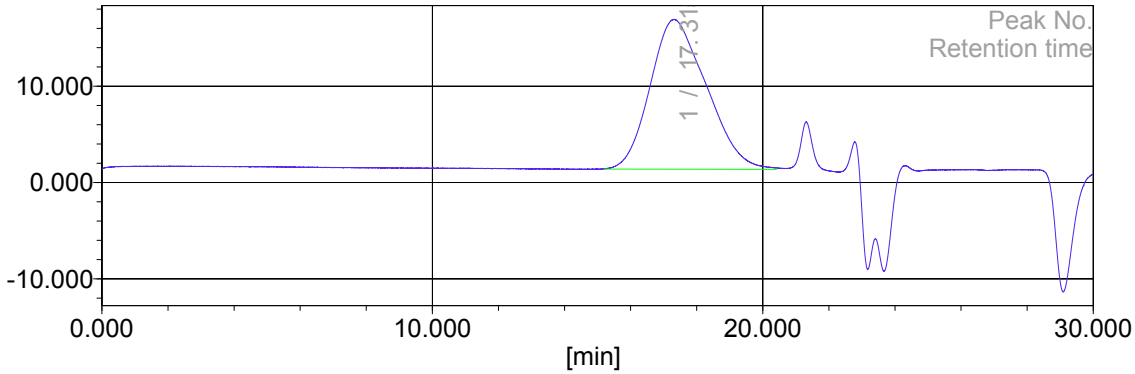

Result of molecular weight calculation (RI)

Peak 1 Valley Peak

	[min]	[mV]	[mol]		
Peak start	15.218	1.431	92,405	Mn	8,878
Peak top	17.315	16.939	15,683	Mw	16,200
Peak end	20.407	1.516	706	Mz	24,463
				Mz+1	32,697
				Mv	16,200
Height [mV]			15.550	Mp	16,758
Area [mV*sec]			1831.665	Mz/Mw	1.510
Height% [%]			100.000	Mw/Mn	1.825
[eta]			16199.87971	Mz+1/Mw	2.018

C_{15} polyester:

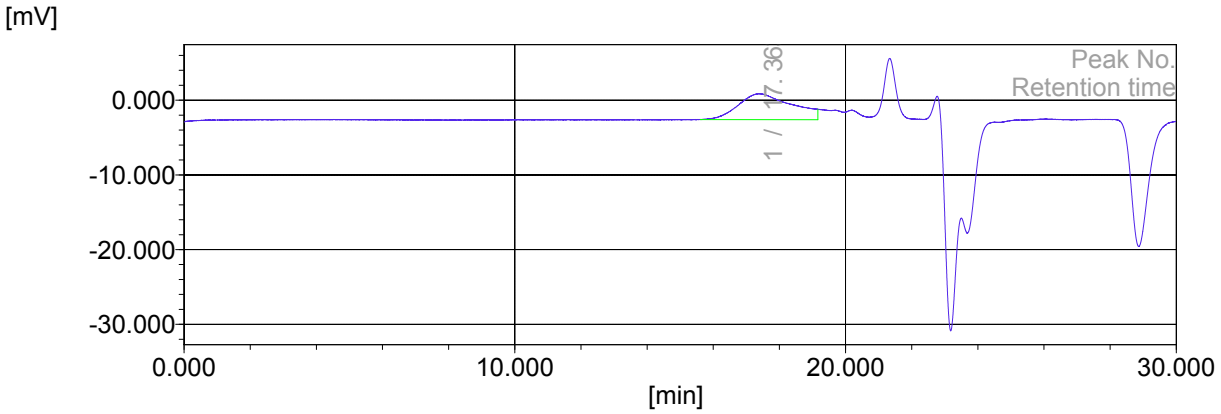

Result of molecular weight calculation (RI)

Peak 1 Valley Peak

	[min]	[mV]	[mol]		
Peak start	15.612	-2.582	68,177	Mn	8,441
Peak top	17.363	0.869	14,977	Mw	13,892
Peak end	19.162	-1.197	2,421	Mz	20,426
				Mz+1	26,707
				Mv	13,892
Height [mV]			3.469	Mp	14,978
Area [mV*sec]			393.546	Mz/Mw	1.470
Height% [%]			100.000	Mw/Mn	1.646
[eta]			13891.82209	Mz+1/Mw	1.922

References:

(1) Dealy, J. M.; Larson, R. G. *Structure and Rheology of Molten Polymers*; Pg 137, 2006.

(2) Razafiarison, T.; Holenstein, C. N.; Stauber, T.; Jovic, M.; Vertudes, E.; Loparic, M.; Kawecki, M.; Bernard, L.; Silvan, U.; Snedeker, J. G. Biomaterial Surface Energy-Driven Ligand Assembly Strongly Regulates Stem Cell Mechanosensitivity and Fate on Very Soft Substrates. *Proc. Natl. Acad. Sci.* **2018**, *115* (18), 4631–4636.

(3) Gentleman, M. M.; Gentleman, E. The Role of Surface Free Energy in Osteoblast–Biomaterial Interactions. *Int. Mater. Rev.* **2014**, *59* (8), 417–429.

(4) Fowkes, F. M. Determination of Interfacial Tensions, Contact Angles, and Dispersion Forces in Surfaces by Assuming Additivity of Intermolecular Interactions in Surfaces. *J. Phys. Chem.* **1962**, *66* (2), 382–382.

(5) Fox, H. .; Zisman, W. . The Spreading of Liquids on Low Energy Surfaces. I. Polytetrafluoroethylene. *J. Colloid Sci.* **1950**, *5* (6), 514–531.

(6) Carré, A. Polar Interactions at Liquid/Polymer Interfaces. *J. Adhes. Sci. Technol.* **2007**, *21* (10), 961–981.

(7) Toussaint, A. F.; Luner, P. The Wetting Properties of Grafted Cellulose Films. *J. Adhes. Sci. Technol.* **1993**, *7* (6), 635–648.

(8) Van Oss, C. J. *Interfacial Forces in Aqueous Media*; Taylor & Francis, 2006.